

Article

Interactive Web Mapping Applications for 2D and 3D Geo-Visualization of Persistent Scatterer Interferometry SAR Data

Panagiotis Kalaitzis ¹, Michael Foumelis ² , Christos Vasilakos ^{1,*} , Antonios Mouratidis ² 
and Nikolaos Soulakellis ¹

¹ Department of Geography, University of the Aegean, 81100 Mytilene, Greece

² Department of Physical and Environmental Geography, Aristotle University of Thessaloniki, 54124 Thessaloniki, Greece

* Correspondence: chvas@aegean.gr

Abstract: Surface motion is a complex, dynamic phenomenon that draws significant scientific attention. This study focuses on the development of a cartographic toolset for the visualization of space-borne Persistent Scatterer Interferometry (PSI) surface motion measurements. The entire archive of Sentinel-1 Synthetic Aperture Radar (SAR) imagery over the broader Thessaloniki (Greece) area has been exploited to derive the PSI measurements utilizing the Surface motion mAPPING (SNAPPING) service on the Geohazards Exploitation Platform (GEP). A collection of web map applications, interactive visualization tools, and an animated map were developed based on state-of-the-art approaches. This geo-visualization toolset consists of the following: (i) Three web map applications exploring PSI velocity rates, PSI time series, and a comparison of PSI with geodetic leveling data; (ii) Two interactive map tools focusing on 3D visualization of PSI time series and estimating velocity rates for predefined temporal frames; and (iii) An animated map of PSI time series. The utilization of the aforementioned visualization toolset provided useful conclusions about the variety of land displacement that occurs in different subareas of Northern Greece from different causes. More specifically, certain subareas with significant subsidence rates range from -2 mm/year up to -18 mm/year from 2015 to 2020. The magnitude of displacement and the underlying causes (subsidence, faults, landslides, human processes, etc.) varies across different subareas. On the other hand, a subarea of uplift trend exists in the north of the city of Thessaloniki with displacements up to 5 mm/year for the period between 2015–2020, despite being constrained by the fact that the geo-visualization platform is able to display SNAPPING PSI measurements from any location around the world, making it a useful tool for global exploration. The platform's contents are available through a user-friendly graphical interface and are mostly addressed to domain experts as well as end-users. Opposed to similar approaches where static 2D maps and velocity rates web applications are presented through this platform, users can monitor and study the dynamic behavior of surface motion to a spatiotemporal extent more thoroughly.

Keywords: web mapping applications; geo-visualization; cartography; PSI interferometry; surface motion; SNAPPING service



Citation: Kalaitzis, P.; Foumelis, M.; Vasilakos, C.; Mouratidis, A.; Soulakellis, N. Interactive Web Mapping Applications for 2D and 3D Geo-Visualization of Persistent Scatterer Interferometry SAR Data. *ISPRS Int. J. Geo-Inf.* **2023**, *12*, 54. <https://doi.org/10.3390/ijgi12020054>

Academic Editors: Wolfgang Kainz and Florian Hruby

Received: 31 October 2022

Revised: 19 January 2023

Accepted: 6 February 2023

Published: 7 February 2023



Copyright: © 2023 by the authors. Licensee MDPI, Basel, Switzerland. This article is an open access article distributed under the terms and conditions of the Creative Commons Attribution (CC BY) license (<https://creativecommons.org/licenses/by/4.0/>).

1. Introduction

The abundance of spatial data, in combination with advances in technology, leads to the development of various digital mapping products. Key attributes, such as speed and the relatively low cost of production, in parallel with the almost real-time visual interaction from the end-user, solidify the advantageous role of these applications. The need for more efficient ways to present and communicate cartographic data has always been a challenge among various fields [1]. This need directed the researchers to focus on the more dynamic aspects of map-making [2], such as the evident transition from distributed types of information delivery to discrete and the domination of wired access over wireless [3].

One of the most distinct types of modern cartographic applications is web mapping, as it enables the process of designing, implementing, generating, and delivering maps on the World Wide Web [4].

Creating and using web mapping applications provides an effective way to present spatial data to domain experts and the general public [5]. Considering the wide spectrum of dataset types and the users' need for multiple and different ways of engagement, the conceptualization of the most optimal visual output is rather crucial [6]. Visualization involves not only representation but also interaction [7–9]. Therefore, a visualization specialist should be able to design and construct graphic representations that encode information about real-world occurrences in a legible and interesting way, as well as graphic interfaces that allow users to alter these representations effectively and efficiently [10].

Ground deformation and instability phenomena are geo-hazards-induced processes that require systematic detection, monitoring, and mapping. Interferometric Synthetic Aperture Radar (InSAR) technology is a mature geodetic imaging technique, which became popular back in the 1980s, and over the course of its development, it has been proven capable of mapping and monitoring ground deformation [11]. Despite being constrained by inherited limitations, similar to all measurement techniques, it offers several advantages compared to other traditional geodetic approaches, such as the Global Navigation Satellite System (GNSS) and leveling. InSAR's advantages include independence from ground installations and long-range coverage at low cost, while obvious shortcomings include the extraction of motion along a satellite's line of sight (LoS) in a single direction, compensation for atmospheric delays, and the spatio-temporal decorrelation effect. The Persistent Scatterers Interferometry (PSI) approach, as a viable extension of InSAR techniques, can effectively compensate for those shortcomings, providing surface motion measurements with millimeter-scale accuracy [12]. The PSI sensitivity to small ground displacements is one of the key advantages of the technique [13], establishing PSI as a widely accepted tool for measuring surface motion, as shown by numerous case studies [14–17].

Recently, a new era of systematic monitoring utilizing SAR sensors has begun since the launch of the first satellite of the Copernicus Sentinel-1 mission on 8 April 2014. Sentinel-1 is a significant advancement over the previous European C-band SAR missions (ESA's ERS and ENVISAT historical missions), as it reduced the temporal revisit time from 35 to 12 days (6 days with two satellite segments) while ensuring large swath coverage of 250 km. As a result of the open and free dissemination strategy for the Sentinel data and the maturity of InSAR techniques, there has been ever-increasing exploitation of spaceborne SAR data for land applications, especially for geohazards [18].

To this extent, the availability of platform-based solutions plays a crucial role in accessing Earth Observation (EO) data and execution of complex algorithms in a user-friendly manner. The Geohazards Exploitation Platform (GEP) is a cloud-based environment providing access to satellite imagery in addition to EO processing services that allow mapping hazard-prone land surfaces and monitoring surface motion. The platform is continuously expanding by integrating a broad range of on-demand and systematic services hosted on cloud resources. Its aim is to contribute to a better understanding of geohazards and their impact through the exploitation of EO services. Among the services offered to users, the on-demand Surface motion mAPPING (SNAPPING) service consists of independent components for the PSI analysis of Copernicus Sentinel-1 mission data. The service has been operational since February 2021, offering GEP users access to an automatic chain for extracting average motion rates and corresponding displacement time series [19].

Currently, with the availability of all individual components, namely operational SAR missions, open and free EO data, and hosted cloud services, users are given all means for the massive production of EO-based results. Still, their interpretation remains a challenging process [20]. Thus, proper visualization of interferometric measurements should be considered a priority, especially to support further investigation and analysis by non-expert users.

In the same context, visualization of the wealth of information ‘hidden’ within PSI measurements is not often the case. Indeed, a large number of published studies involving PSI or other multi-temporal InSAR techniques are limiting their analysis and visualization to static 2D maps of velocity rates [21–25] with no special attention to corresponding displacement time series. On the other hand, well-configured interactive web-map applications exist, such as the European Ground Motion Service (EGMS) [26] and the Norwegian Ground Motion Service [27]. However, they are developed for specific pre-processed data and not as stand-alone tools to be used with the other sources of the measurements.

It is thus clear that even though the rate of EO practitioners utilizing PSI measurements keeps increasing, there is a lack of well-tailored visualization tools for the proper exploitation of these geodetic datasets. Therefore, the availability of open-source interactive cartographic tools for visualizing the totality of information provided by a PSI dataset in a user-friendly manner is required. Interactive geo-visualization tools can be proven critical and decisive components in visualizing and exploring PSI datasets. Using those tools may enhance comprehension and interpretation of multi-temporal datasets. By using one open-source geo-visualization toolset, domain experts, as well as end-users, are given the means to perform collective operations benefiting decision-making processes.

The aim of this study is to present a newly developed interactive toolset in support of EO practitioners, providing access to different cartographic approaches for the visualization and exploitation of spaceborne PSI measurements. The toolset includes visualization web map applications focusing on exploring PSI velocity rates and PSI time series and comparing PSI data with leveling data. It also contains an animation video for exploring displacement values of a PSI time series dataset through time. Finally, it provides two interactive visualization tools, contributing to the 3D visualization of time series of PSI data and estimating velocity rates of a predefined time interval. To the best of our knowledge, stand-alone, open-access, interactive tools have not been presented yet for visualizing all derived data of a PSI dataset.

2. Study Area

The study area of this research refers to the northern Greece region that entirely covers the city of Thessaloniki, Koronia Lake, some of the major rivers, such as Gallikos, Axios, Loudias, Aliakmonas, and Anthemountas, the Thermaikos gulf, and the Koronia-Volvi National Park (Figure 1). Elevation ranges from 0 m in coastal areas up to 1196 m on mount Chortiatis, and the whole area of the region is about 500 km².

The geological setting lies within the Axios–Vardar geotectonic zone and Circum Rhodope Belt of internal Hellenides. They are characterized by a complex tectonic history and alternating lithostratigraphic units with the evident presence of ophiolitic complexes. In particular, the Axios–Vardar zone consists of NE dipping thrust sheets, with an NW–SE strike, dominated by the presence of metamorphic and deep-sea sedimentary rocks [28], while the neighboring Circum Rhodope Belt is characterized by repeated SW-directed thrust sheets consisting of sedimentary, igneous, and various types of metamorphic rocks [29,30].

Over the past years, several InSAR studies have been conducted over the study area, successfully quantifying ongoing subsidence phenomena [31–34]. Since 1991, vertical deformation phenomena have been detected, with the highest subsidence rates located in the Kalochori–Sindos–Chalastra region, Mygdonian Basin, and Anthemountas Basin. Motion rates reach -15 mm/year, varying depending on time interval and subarea under consideration. Some of the applications and tools created herein were evaluated on the part of the aforementioned regions exhibiting high displacement gradients, namely the broader Sindos region.



Figure 1. Area of interest located in the north part of Greece, referring to land included within the red line, bounding box. Base map source: Esri, GEBCO, DeLorme, NaturalVue, Garmin, FAO, NOAA, USGS.

3. Materials and Methods

The methodological part of the study can be divided into three main components:

1. Data Acquisition, describing the SAR and the leveling data used;
2. Data Processing, detailing the techniques implemented for processing the SAR imagery as well as their post-processing as part of their preparation for further cartographic analysis;
3. Geo-Visualization, referring to an animated map, cartographic tools, and 2D layers properly visualized that contribute to the web map creation.

Finally, a geo-visualization toolset is developed, consisting of an animated map, three web map applications, and two interactive visualization tools. Each of the geo-visualization toolset elements contributes to the efficient and valuable visualization and diffusion of ground motion data. The methodology is based on the flow chart presented in Figure 2.

3.1. Data Acquisition

The entire archive of Sentinel-1 Single Look Complex (SLC) data used consists of 138 SAR images acquired along descending track 7, well-distributed over a period of approximately 6 years (between April 2015 and December 2020). The preference for the descending orbit was due to the fact that for the specific acquisition time (at about 04:30 UTC), the influence of the atmosphere and ionosphere was relatively lower.

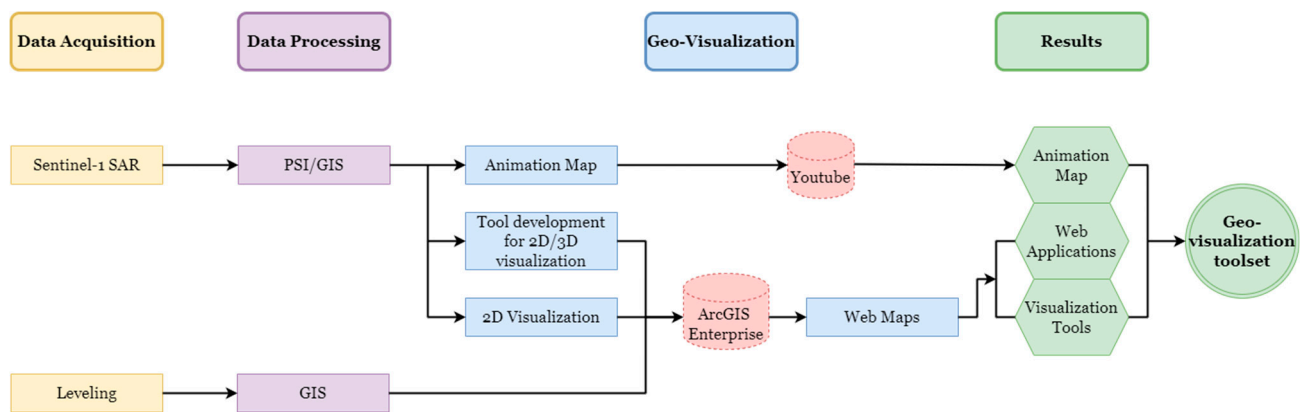


Figure 2. Workflow of methodology followed for the integration of the research.

Additionally, the leveling data was available for the period between June 2018 and June 2020. Leveling is a precise and time-consuming procedure by which the height differences between the neighboring points can be measured with sub-centimeter precision [35–37]. Spirit leveling was conducted in the broader area of the Sindos region. Leica DNA03™, a high-precision digital level with a nominal accuracy (standard deviation per kilometer double run) of 0.3 mm, was the instrument utilized for the measurements. A network of 11 points was established in the study area, and a reference point was located outside the deformation-affected area. The data reveals the diachronic occurrence of subsidence in the Sindos region, while some investigations have detected significant uplifts. According to these reference data, a total vertical displacement trend of up to -15 mm for the first year of measurements between 2018 and 2019 occurs. In the second period (June 2019–June 2020), the majority of values are determined by relative stability, and the remaining few values are characterized by a significantly lower displacement (subsidence or uplift).

3.2. Data Processing

The interferometric processing of the Sentinel-1 data was performed using the SNAPPING service on GEP. Specifically, SNAPPING Interferogram Generation (IFG) service was run for the generation of the interferometric stack, a collection of single reference differential interferograms stored on the platform resources for further analysis. This IFG stack was then inserted as input for the actual time series analysis through the SNAPPING PSI service. SNAPPING PSI was run at medium spatial resolution (PSI Med) since a relatively large area was considered (approx. 90×90 sq. km). At medium resolution, identified Persistent Scatterer (PS) targets were merged, over a 100 m search radius, based on specific criteria, thus reducing their numbers over regions of high point densities. As a consequence of the reduced point density, SNAPPING PSI Med allows for the decrease of computational time and resources required for the processing. Since our work focused more on the post-visualization of PSI measurements and not on the detailed mapping of surface motion, medium-resolution results were considered adequate for our demonstration purposes.

Following the completion of PSI processing, measurements come in delimited text format, specifically as a CSV (comma-separated values) file, which includes information about coordinates, velocity, velocity sigma, temporal coherence, heights, and incident angle, as well as the displacement time series for each of the points. The velocity and velocity sigma attributes refer to the average LoS displacement rate and the corresponding standard deviation, respectively, both measured in mm/year. A PSI time series is associated with a single point measurement and depicts the displacement history of that Persistent Scatterer (PS) target through time, starting from the initial acquisition date [26].

The incorporation of the measurements on the geodatabase server is achieved through the conversion of the CSV file into a GIS-suitable format (shapefile). In that way, each one of the points consisting of that file will be located by its coordinates but will also provide all the above-mentioned information, such as velocity rates and time series displacement.

This specific PSI dataset consists of almost 44,000 geolocated PSs with 138 acquisitions between 2015–2020. Thus, the whole dataset contains more than 6,000,000 registrations. A similar process is conducted on leveling data. Leveling measurements refer to the height differences in geolocated points. Leveling output dataset is converted from CSV file to shapefile so data can be readable by the server and also be comparable with PSI data.

An important point that has to be examined is the time contained in PSI data. For this purpose, time is presented in columns at the attribute table, in two ways, as a date (ex. 30 June 2020) and as a decimal date (ex. 2020.4955). Transforming date into the decimal date gives the opportunity of using dates of time series in equations. Our dataset contains 138 unique dates (referring to every SAR image processed) from 4 October 2015 up to 27 December 2020, with no equal time interval between them.

3.3. Geo-Visualization

The first and probably one of the most crucial aspects that had to be examined at this stage was the cartographic scale. Spatial data might provide varied information about the examined features and their relationships depending on the scale used [38]. The cartographic scale should be prefixed, and the symbol size of PSI data (point vectors) should be adapted on every different scale. By this categorization, it is easier for the viewer to have a better overview of the data. Prefixed cartographic scales that were used for these data are as follows:

1. 1:1,000,000, covering the whole study area, correlated with the extent of a SAR satellite image;
2. 1:500,000, able to present PSI data over extensive geomorphological units, such as lakes, mountains, rivers, etc.;
3. 1:250,000, suitable for the presentation of PSI data covering municipalities and big cities;
4. 1:100,000, providing a sufficient depiction of PSI data over cities and villages.
5. 1:50,000, able to provide information on PSI data over big human structures such as airports, bridges, etc.;
6. 1:25,000, providing presentation of PSI data even over smaller areas, such as rural areas and settlements;
7. 1:10,000, suitable for presenting PSI data over different sizes of public road networks;
8. 1:5000, able to present PSI data on building blocks;
9. 1:2500, for neighborhood or building-based scale presentation of PSI data.

Scales 2, 5, 6, 7, and 8 are also compatible with cartographic scales used in geological and topographic maps provided by the Hellenic Military Geographical Service and Hellenic Authority for Geological and Mineral Surveys.

Symbol size was adjusted accordingly to every unique chosen scale, bigger-sized symbols for smaller cartographic scales (1, 2, 3, 4, 5) and smaller-sized symbols for big cartographic scales (6, 7, 8, 9), respectively. All cartographic scales mentioned are presented in Figure 3.

The second aspect involves the classification of quantitative data that provides a better visual representation of the PSI velocity field by the cartographic method of the graduated symbol. Velocity rates present average LoS displacement in mm per year. For this specific data set, the min value is -17.5 mm/year, and the maximum value is 7.6 mm/year, where most of the values occur on the value interval of ± 3 mm/year. In order to approach the most suitable cartographic method for visualizing PSI velocity data, five classification methods were applied to the same data set. These methods are as follows: Equal Intervals (1 mm/year for each class); Equal Intervals (2 mm/year for each class); Quantiles; Natural breaks; and Stretched method. The evaluation of the classification method is based on how well each technique meets various criteria, such as smooth fluctuation between velocity rates of displacement, demarcation of deformation or none-deformation zones, visualization of extreme values, and feasible comparison with other corresponding research. Each one of them has advantages and disadvantages, depending on the different

usages of each map. Three of them display a satisfactory visual representation of velocity displacement rates. The cartographic results of all other techniques were considered unsatisfactory because they did not present sufficient distribution of data, resulting in not fulfilling the above-mentioned criteria; therefore, they have been excluded from the evaluation process. The three most suitable cartographic techniques are Stretched, Equal Interval (one mm/year for each class), and Natural Breaks, as shown in Figure 4. The employed classification methods shown in Figure 4a–c are the most suitable classification methods for velocity rates of PSI data depiction, presenting good distribution of data and fulfilling the above-mentioned criteria. The Stretch Method shown in Figure 4a is proposed as the most suitable approach for visualizing velocity rates of PSI data. Although the equal Interval Method (Figure 4d) shows a sufficient distribution of data, there is not a smooth fluctuation in velocity rates. The quantiles classification technique (Figure 4e) does not adequately distribute the data, and the visualization of extreme values is unclear.

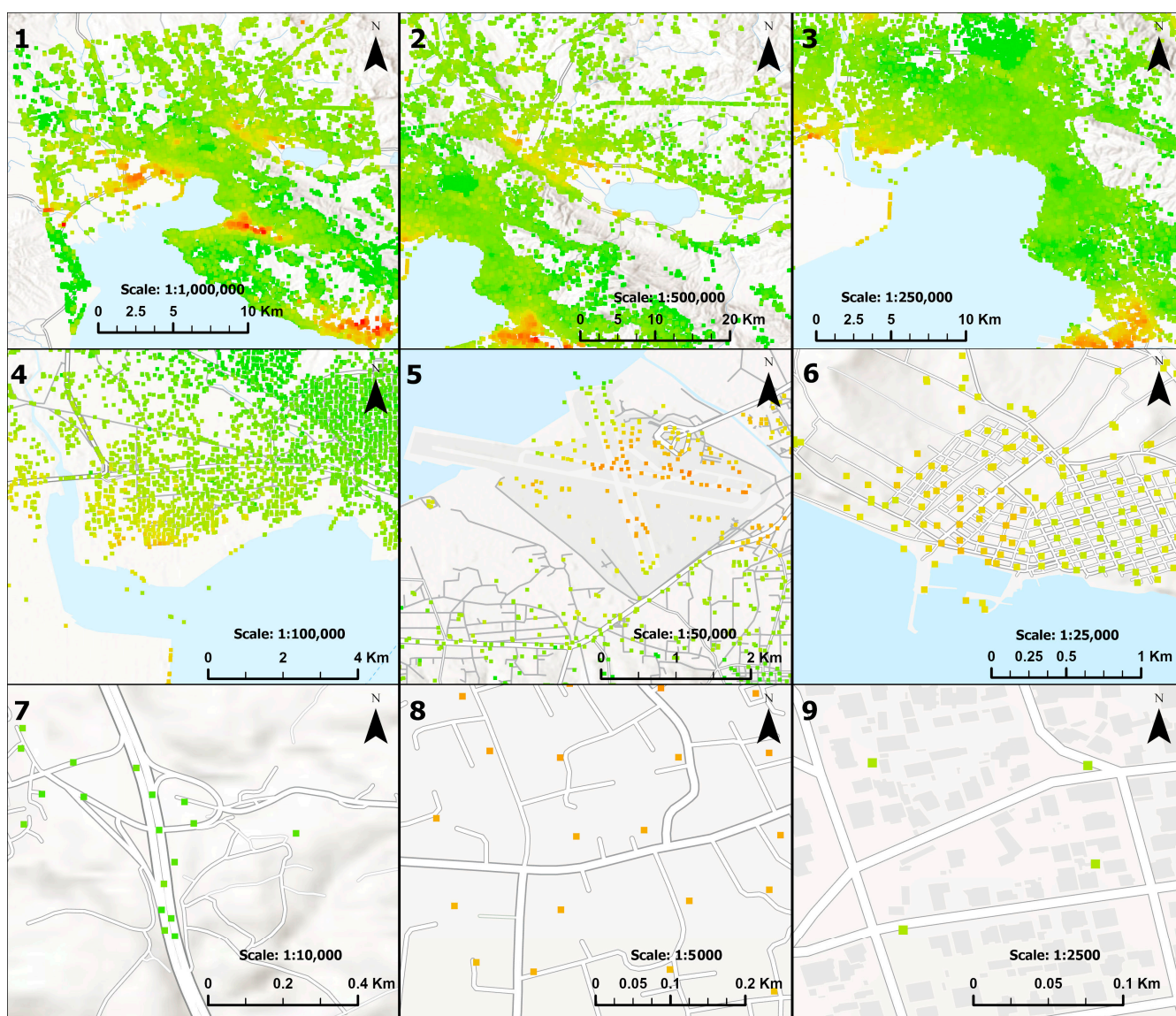


Figure 3. Categorization of the nine different prefixed cartographic scales used for presenting PSI data.

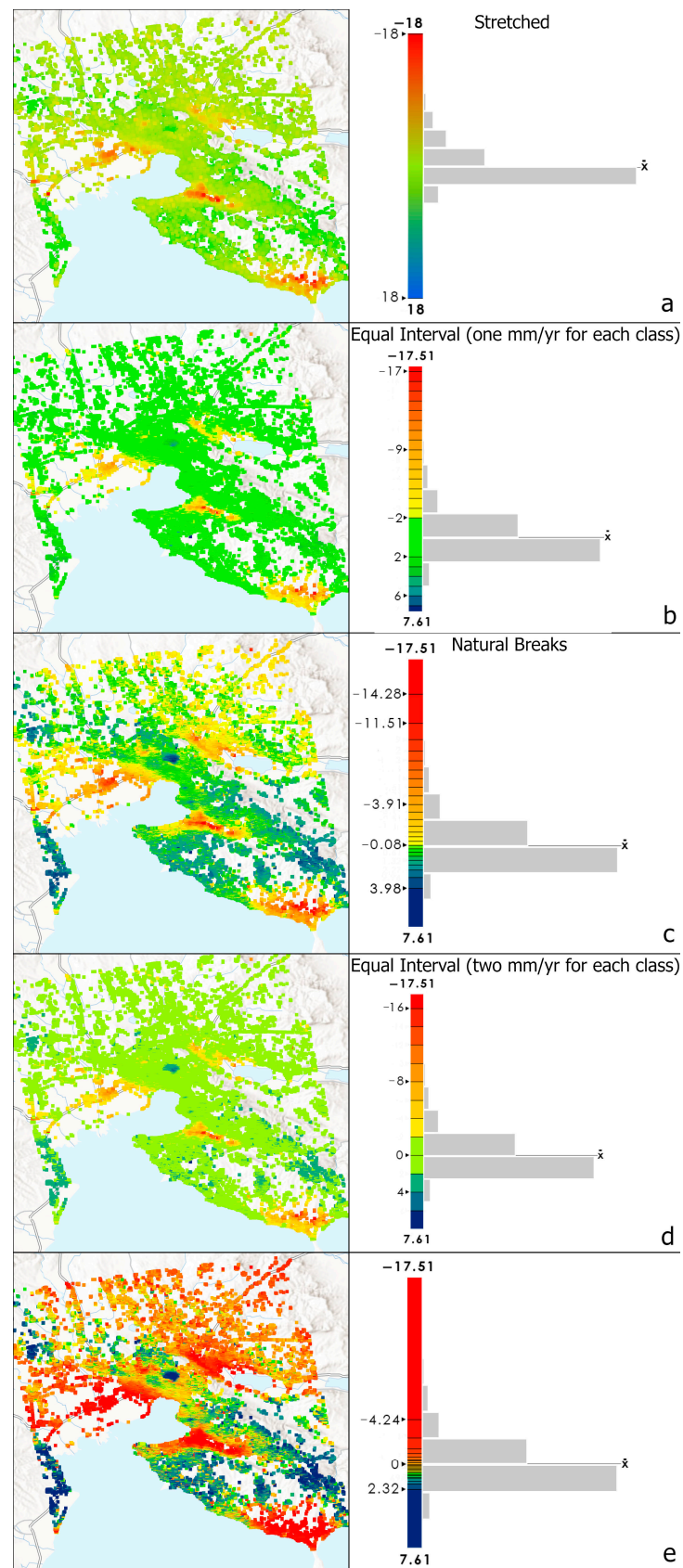


Figure 4. All five cartographic techniques i.e. (a) stretched, (b) equal interval (one mm/year for each class), (c) natural breaks, (d) equal interval (two mm/year for each class) and (e) quantiles were evaluated on the same dataset. Cartographic results are presented respectively by their velocity values contributions and color pallets.

3.3.1. 2D Visualization to Web Maps

The field of web cartography is constantly evolving and improving with frequent updates and technical advancements [39–41]. During various stages of PSI data processing, web-based GIS can play a crucial role in the collection and dissemination of essential information in a rapid, relatively inexpensive, and clear manner [42]. In order to manage (store, process, visualize, and share) all of those data, the ArcGIS Enterprise geodatabase server was used. For efficient visualization of velocity rates, time series displacement values, and leveling data (points), three web maps have been created:

1. The velocity web map, presented in millimeters per year, visualizes the mean velocity rates of the study area for the period between 2015–2020;
2. Time series web map, visualizing the displacement values in millimeters of the study area. Each point of the data set includes information on the displacement value of every intermediate date between 2015–2020;
3. Leveling data web map presents time series values of PSI data combined with leveling-derived displacement values. Both datasets present displacement in millimeters for the period of June 2018–June 2020.

Those three web maps have been used to create interactive web applications.

3.3.2. Animated Map

A cartographic animation is an expressive form of dynamic visualization in the context of spatial data management, allowing for the display of exceedingly complex processes. Geospatial data animations can display changes in space (position), location (attribute), and time [1]. One of the most common ways to visualize temporal point data is by creating an animation video [43]. During this study, an animated map presenting displacement values from 2 May 2015 to 19 March 2021 of the study area was created. The animated map created also contains elements of a common map, such as a title, orientation, and legend. The date is also presented as an active field corresponding to the data presented on the animated map. The animated map was finally uploaded to YouTube™, making it accessible to all users of the geo-visualization toolset.

3.3.3. Tool Development for 2D/3D Visualization

In order to visualize and interactively explore the InSAR time series, two interactive map tools were developed: (i) an interactive 2D tool that estimates and visualizes velocity rates for predefined time frames; and (ii) an interactive 3D exploration and visualization tool of time series, presenting every intermediate value of displacement of the point dataset.

Furthermore, by working on the visualization of the velocity data, we realized the need to estimate the velocities of each point on smaller periods and areas. Velocity estimation for each point comes from calculating the slope of the linear regression between the single displacement value and time. The main idea here is to re-estimate the slope velocity of every single point of the data set for smaller time frames in different subareas of interest. If the acquisition period or the observation time window changes, then the velocity rate of each point is also affected. Based on the latter, an ArcPy script was developed, which automatically estimated the velocity rates of points depending on the studied time interval within the time frame range of the original dataset. Velocity rates of each point of the dataset are estimated by the linear regression between displacement values and time.

The first step was to isolate the subarea of interest by selecting and extracting all points that are enclosed within. Then, we transformed the date into a decimal number, so it could be in the proper format in order to be part of a linear regression. Additionally, we created a new null column on the attribute table of the shapefile in order to store every new estimated value. Then, we added a slide bar of time, which expanded the time range of the data set. In the next step, we encoded a script that worked as a loop by estimating the velocity of the data (depending on the time selected) set and overwrote the results on the newly created file. Finally, the user has the option to define the time range of interest by the time slider and then call the script created. Data for this tool are shared as a layer

package, so users are able to download and open it on ArcGIS Pro. Subsequently, they should also download the supplementary script as a text file, then paste it and run it on the ArcGIS Pro notebook. Then, by looping from point to point, the velocities of every point of the dataset are calculated and visualized (by refreshing data) on a predefined color pallet similar to the one used for visualizing the velocity of PSI measurements (from blue to red when uplift or subsidence, respectively). Users also have the option to manually select a point by id and have a graph of all its displacement values through the selected time frame, which represents the linear regression line that refers to its mean velocity value. By clicking on graph properties, users have the option to see the equation of linear regression that estimates the mean velocity of each point. The value of the velocity rate for this specific point is also written on the new field created on the attribute table. Overall, the script became a useful tool that generated mean velocity values depending on any time frame and subarea needed.

When visualizing PSI data over a study area, the main visualized variable is velocity [13,18,44,45]. When exporting the PSI data per PS target, there is also information about individual displacement values corresponding to the satellite acquisition dates. This information is crucial to the study because of the evolution of motion for each PS through time. Usually, it can be represented by using time slider bars on 2D maps or a series of 2D maps. The need for immediate visualization of this useful information led to a 3D visualization approach, where the third dimension refers to time. This visualization is achieved via colored tiles (depending on displacement value) that expand on the z-axis above every point of data. The idea for this approach stems from the space–time cube representation that has been widely used for the simultaneous display of time and spatial data.

This visualization tool also provides sliders that give the opportunity to select period and displacement value ranges. When users make a selection with these sliders, the corresponding tiles are depicted in the final visualization. Finally, by selecting a random (on time and location) part of that space–time cube, a graph is created that illustrates displacement values through time. If one point of the data set is selected (by id), then the created graph refers to the evolution of this point for the exact selected period. If more than one point is selected, the presented graph automatically splits all points by id into different colored lines for the selected period. A complete interpretation of the evolution, through time, of the displacement values is given by also using a 3D navigator, as well as time and displacement values slide bars. This tool is also shared as a layer package, so there is a need for specific software in order to download and experience it.

3.3.4. Web Map Applications

Gehlot and Hanssen [20] refer to the importance of a clear view and understanding of ground deformation data (such as those pertaining to land subsidence) by authorities and other relevant bodies. However, the PSI data processing technique is sometimes too challenging for a “non-expert” in the broader user community. In order to bridge this gap between PSI measurements and end-users, they used Geographical Information Systems (GIS) that could work as an interactive tool to visualize and analyze radar time series data. Moreover, a Web-GIS interactive visualization interface was developed to communicate PS-derived land subsidence data to end-users.

Following the same concept, through ArcGIS Web App Builder™, we created three web map applications that work as cartographic tools in order to visualize and provide a full and clear perspective of ground displacement PSI measurements. These three web map applications, i.e., (a) a PSI velocity rates web map application, (b) a PSI time series web map application, and (c) a PSI vs. leveling web map application, are analytically described henceforth.

The PSI velocity rates web map application focuses on visualizing LoS mean velocity rates (mm/year). Users are able to explore the area of interest and examine velocity rates per point by clicking on the respective point and retrieving all relevant information (latitude, longitude, velocity, velocity sigma) on a pop-up window. The application offers the option of using a toolbar, including crucial information about the dataset, such as legend, all

layers loaded, and general processing information. By using this toolbar, users have the option to load further supplementary data. These data could be imported from each user's personal repository or via a URL (if loaded on the geo-server). Hence users practically have the flexibility to load any available online data and investigate the possible correlation with the PSI velocity information. Additionally, with the "selection tool" available in the toolbar, users can select (by polygon) an area of interest and save it as a new layer. This layer can then be studied individually by means of its attribute table or optionally used in conjunction with the "analysis tool", where tools such as buffer creation or point interpolation (for continuous layers) are available. Using analysis tools provides the option of a dynamic statistical analysis process that could lead to drawing immediate conclusions for the selected area of interest. All the analysis tool outputs can be saved on the server and loaded again in the application as new layers. Moreover, the "filtering tool" provides the option for defining upper and lower velocity values thresholds as well as velocity sigma in mm/year. Land use types for each point provided through the ESA Land Cover 2020 dataset [46] are merged with the primary PSI data file. Users also have the option of filtering data points based on the corresponding land use. After defining the desired parameters, points are filtered, and only those points that fit the selection criteria are depicted on the map. The application also provides the option of loading the attribute table of the dataset so that users can zoom in on points by selecting specific lines of the table and sorting data by a specific column.

The PSI time series web map application supports the visualization of PSI time series data. Every displacement value for each unique date is presented in order to visualize the evolution of those values in time. A toolbar is also available here, through which users can retrieve general dataset information and also see the legend and the layers used. Users have the same options for adding and selecting data as well as creating sub-layers from all selected subsets. The most important tool here is the time slider tool, used to define and visualize data corresponding to specific dates. The results of the visualized data refer by default to the last available date. There is also an option for the continuous presentation of all intermediate dates by defining the step interval between dates using the "play" button on the time slider tool. Users also have the option of configuring the sequence speed of each consecutively presented result. For this tool usage, a slow presentation speed is advised so that all data are correctly rendered on the map. Working with a very large amount of data (almost 6,500,000 points) is a challenge and computability-demanding procedure for rendering and visualizing. That is one of the reasons why animated video visualization was also created.

Users finally have the option of using the filtering tool, by which they can select a specific date in order to have the corresponding data as a map result. The main precondition here is that the selected date corresponds to a date where data actually exist. In order to support this selection, the attribute table is also available so that users can have an overview of every available date.

The PSI versus leveling web map application is about comparing displacement values coming from two different methods. The methods used for this comparison are PSI (Persistent Scatterer Interferometry) and leveling. Leveling is quite a demanding procedure in terms of time and manpower; hence, it was conducted in a smaller subarea of interest. A network of 11 stable points was established in this subarea of the Sindos region and measured during the period between June 2018 and June 2020.

As per the previously presented applications, options, such as legend, layer list, and general information presentation, are available in the main toolbar of the application. Users have the option of applying filters on PSI or leveling points in order to study them separately. A time slider is also available for both data sets. The main tool of this application is the chart creation tool, through which graphs of the evolution of displacement values for each point of both datasets can be generated and compared. Users are able to select points of the data set by spatial filters, e.g., by zooming on a specific map area and creating a chart for the points included within this area or by creating a predefined shape (point, line,

polygon circle, etc.) that includes the points of interest. Subsequently, a graph is created, and users have the option to change its parameters, such as color lines, axes, and legend, as well as to enlarge it.

Through this procedure, users are in a position to create graphs for each of the points of the datasets and can, thus, have a better understanding of the evolution of their displacement through time.

3.3.5. Geo-Visualization Toolset

A geo-visualization toolset that includes all web map applications, interactive visualization tools, and an animated map was created so that users could collectively explore them. Each element of that cartographic toolset is presented by its title and can be accessed by selectable previews that work as eligible links. Web map applications are uploaded on the geo-server, and animation map is uploaded online on YouTube. Both are directly accessible, to all users, by clicking on each preview/link of the toolset. Cartographic tools are shared as web layers, where users can click on their previews and download them automatically in the exact same configuration environment as the one they have created.

4. Results and Discussion

4.1. Animated Map

In order to have a quick overview of the PSI displacement time series of the whole study area, an animated map that visualized those values was created. It is a video of approximately 40 s, at a scale of 1:900,000, that continuously presents all PSI displacement time series from 2015 up until 2020. For a quick and efficient illustration of such a long-term phenomenon, the time frame interval of each of the 138 acquisition dates was adjusted to 0.28 s. In the video margins, the title, legend, scale, and active (currently shown) date are indicated. With the aid of this animated map, it is possible to study the evolution of displacement through time. Its values appear to have a negative trend, especially in the aforementioned subareas, although most of the broader study areas seem to be generally stable.

Overall, users have the option to pause the animation video on demand and obtain a static map of displacement for the whole study area for every available date. All this information can be selected and compared for multiple dates, depending on the user's needs. A preview of the animated map is presented in Figure 5.

The entire dataset displays a wide range of deformation values (40 mm to -80 mm), so stretched method was selected on a color ramp from red to blue (negative to positive values) for visualization. The prefixed scale provides an effective interpretation of overall temporal displacements that prevail in the study area.

4.2. PSI Velocity Rates Web Map Application

The PSI velocity rates web map application can be used for exploring PSI velocity rates over a study area. Users have the option to filter points by velocity rates, velocity sigma, and land use. This web map application also provides the option to load any other available layer and compare it with PSI velocity rates. In order to further investigate the spatial distribution of data, users can also apply analysis tools, such as buffer layers and interpolated layers generation. An example of this application usage is presented in Figure 6.

By using this web map application, not only visualization but also an exploration of PSI velocity rates is available. By exporting all dataset values as a layer, a map was created, where four main subareas showing land subsidence (negative surface motion rates) are shown. Those subareas are depicted in Figure 7: (1) Sindos–Kalochori–Chalastra region, with a minimum velocity rate of -11.6 mm/year and a maximum of 2.5 mm/year; (2) The NW part of lake Koronia lake with a minimum velocity rate of -7.6 mm/year and a maximum of 2.5 mm/year; (3) The broader area of Thessaloniki airport, with a minimum velocity rate of -16.1 mm/year and a maximum of 3.0 mm/year; and (4) The broader area of Moudania region, with a minimum velocity rate of -16.7 mm/year and a maximum of

3.0 mm/year. In these subareas, similar motions seem to occur, as indicated by the many independent research endeavors throughout the years [31–33,47–51].

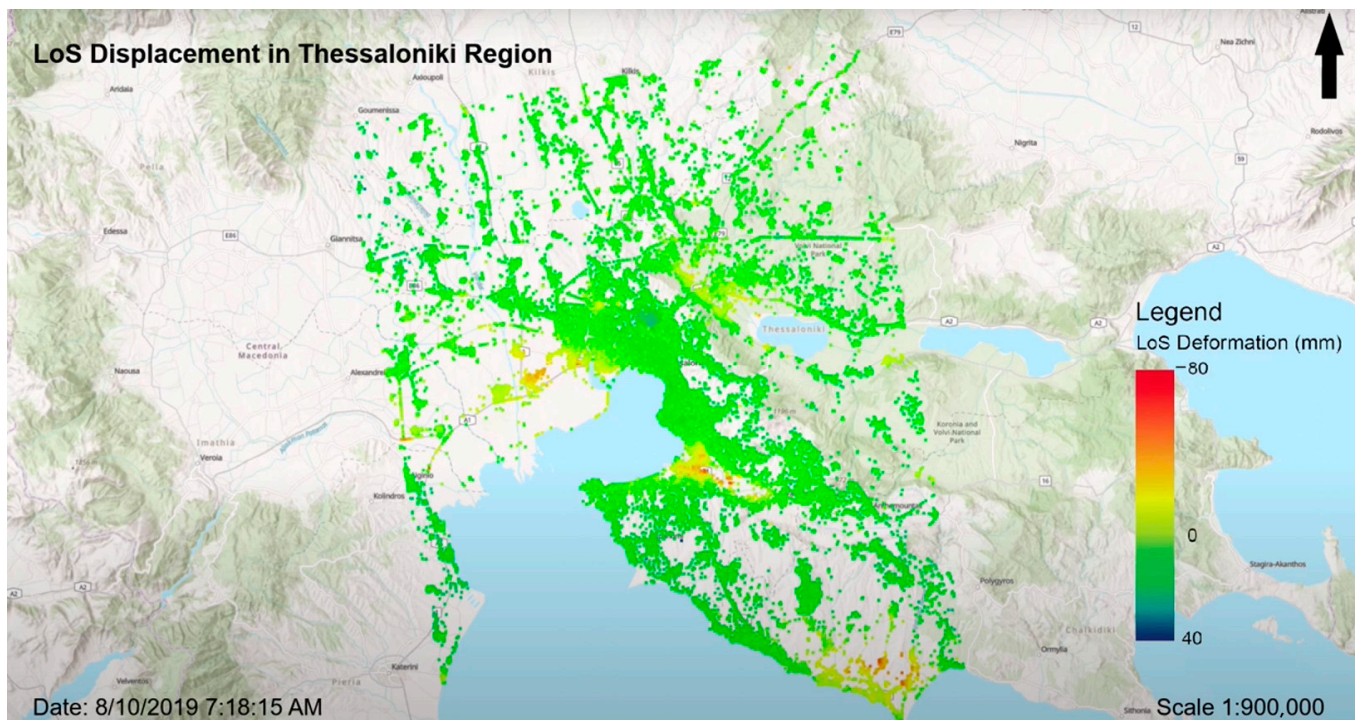


Figure 5. Animation map, with all PSI time series displacement values, presented from 2015 to 2020 in the broader area of Thessaloniki Region. Date presented here is 21 January 2019.

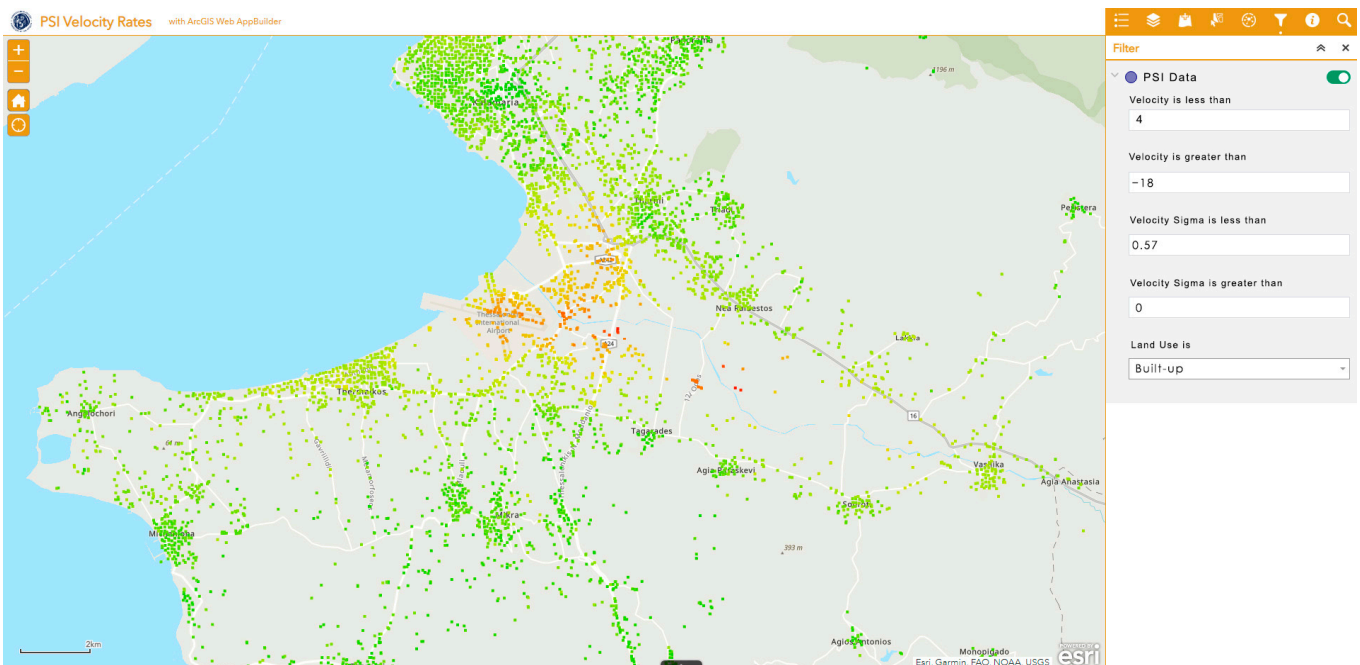


Figure 6. PSI velocity rates from 2015 to 2020 in the broader area of Thessaloniki International Airport, northern Greece. Velocity rates range from 4.0 to −18.0 mm/year and refer to points that are located over buildup areas.

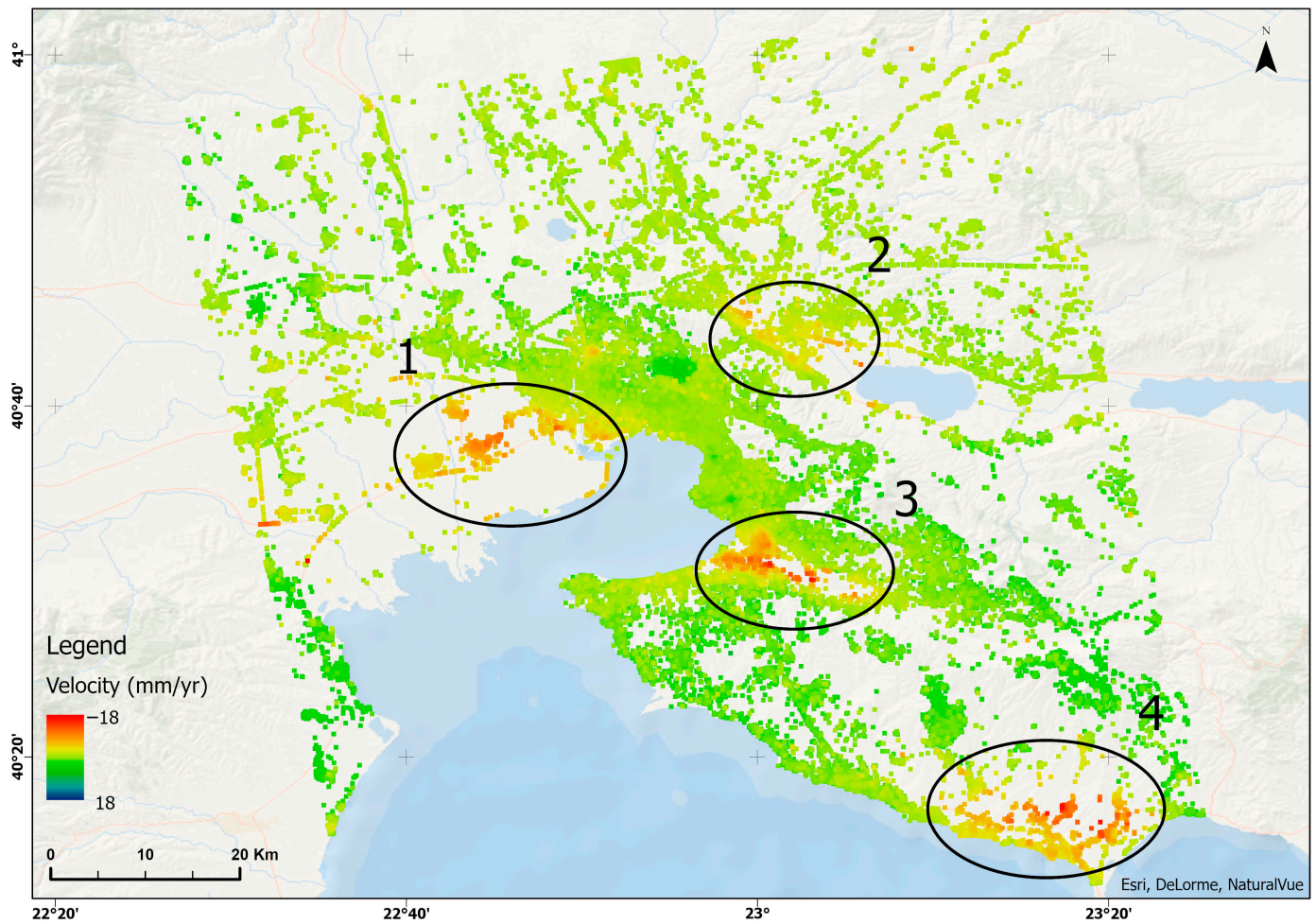


Figure 7. Subareas of (1) Sindos–Kalochori–Chalastra region, (2) the NW part of lake Koronia lake (3) the broader area of Thessaloniki airport and (4) the broader area of Moudania region with negative displacement velocity rates from 2015 up to 2020. Base map source: Esri, DeLorme, NaturalVue.

The first cartographic challenge we had to face was scale and symbol size. We suggest that available scales when visualizing PSI data, should be predefined (depending on the study area), and point size should be alternated in accordance with the selected scale. Through this approach, visualization becomes more efficient and accurate on every different scale selection.

The second challenge we had to overcome was the selection of the cartographic method and color ramp for the optimal visualization of PSI velocities. The stretched method is suggested, with a color ramp from red (negative values) to blue (positive values). The goal here is to achieve an equiponderant color ramp.

4.3. PSI Time Series Web Map Application

The PSI time series web map application can be used for filtering and visualizing PSI time series data of each intermediate date. Users have the option of selecting a specific date of interest and visualizing displacement values over the study area. A preview of this web map application is presented in Figure 8. The selected date in this figure is the 10th of February 2020. Displacement values vary from -40.6 mm up to 34.34 mm relative to the first data acquisition date. The lowest displacement values are mostly presented in the NW of Koroneia lake, whereas the highest displacement values are mostly located on the S part of the subarea.

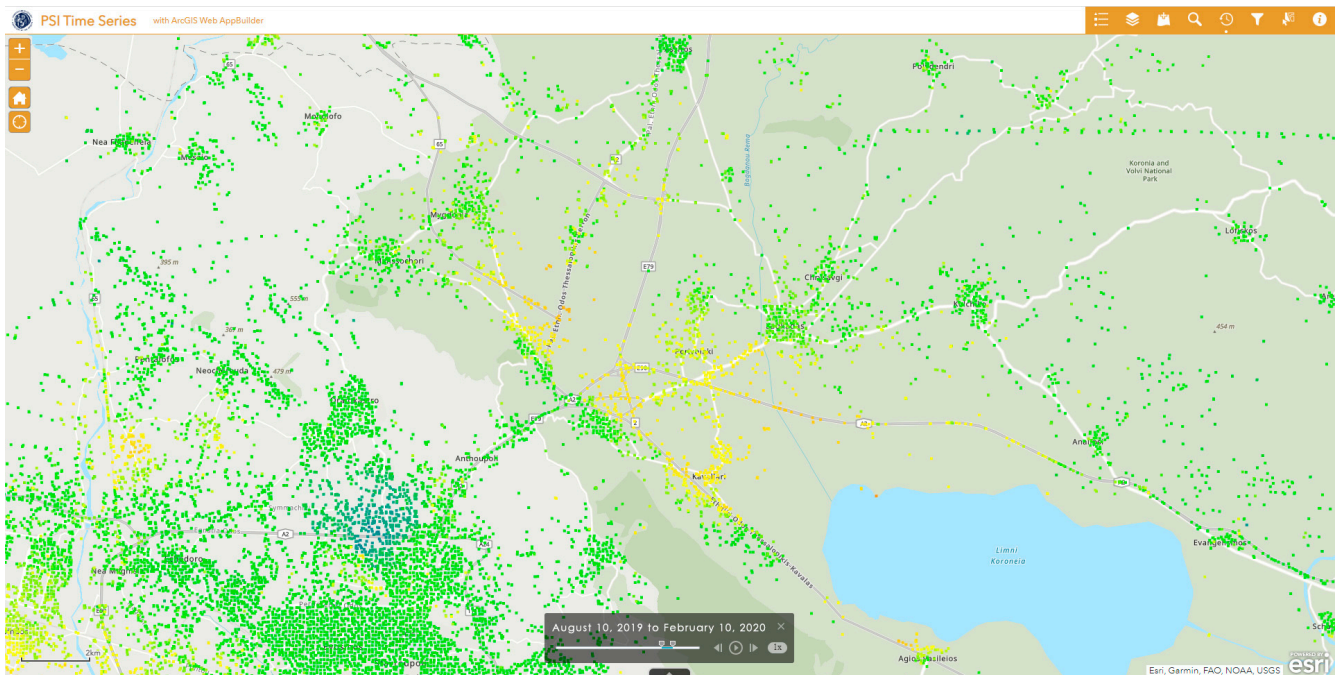


Figure 8. Evolution of deformation web map application, presenting deformation values of unique dates (in mm) in a subarea NW of Koroneia lake.

One of the limitations of this web map application is the large amounts of records loaded. That is why users have the option to select the time and location-based subsets and export them as a new layer. By using this web application, users have the option of extended and detailed exploration of deformation values on specific dates and subareas.

4.4. PSI Versus Leveling Web Map Application

PSI versus leveling web map application focuses on comparing PSI time series data against leveling ground displacement data. Users have the option to explore values of displacement of two different datasets and also to create graphs for the comparison of land displacement trends and values of adjacent points. By using the application and comparing the two methods, the correlation between the two datasets is evident. A general presentation of the web map application interface is presented in Figure 9. Eleven leveling points from this dataset are presented as rhombuses with black outlines, whereas all other points refer to the PSI dataset. The NE leveling point (Figure 9) is used as the reference point during the field measurements. The majority of points present subsidence trend values from June 2018 to June 2019 and more stable or even uplift trends between June 2019 and June 2020. An example of graph generation between adjacent points of different datasets is presented in Figure 10.

The direct comparison of PSI and leveling displacement trends correlates successfully as both graphs follow similar fluctuations in terms of subsidence and uplift rates (Figure 10). The nature and limited time interval of the leveling procedure result in a more linear and simpler trend (i.e., only three timestamps), always in complete agreement with the general gradual fluctuations of the PSI trend. One of the limitations of this web map application arises from the availability and acquisition of leveling data. Leveling is quite a demanding procedure that has to be conducted in the same location and time extended with the available PSI data so both datasets are comparable and visualized simultaneously.

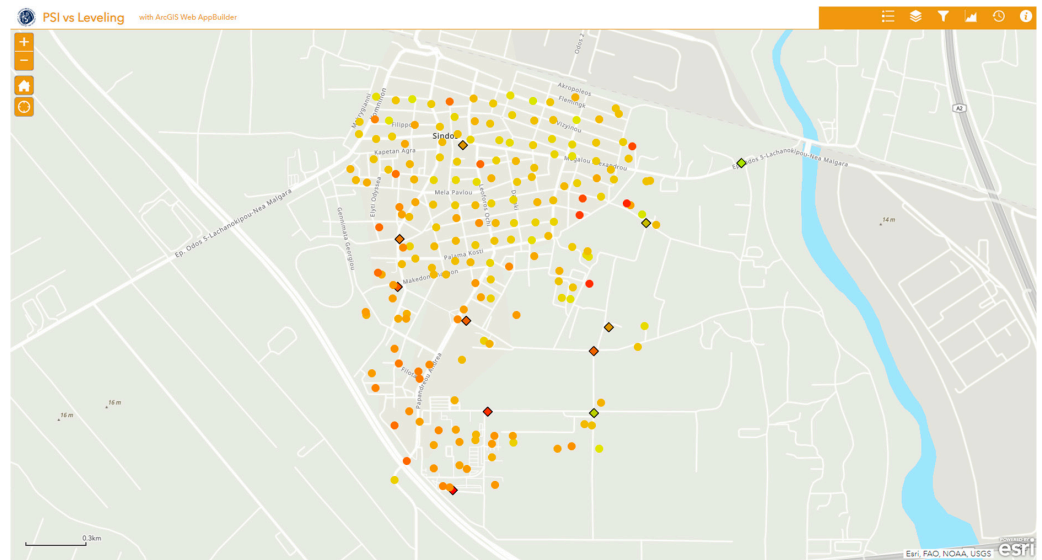


Figure 9. PSI vs. leveling method comparison web application, with two datasets of points depicted over Sindos region.

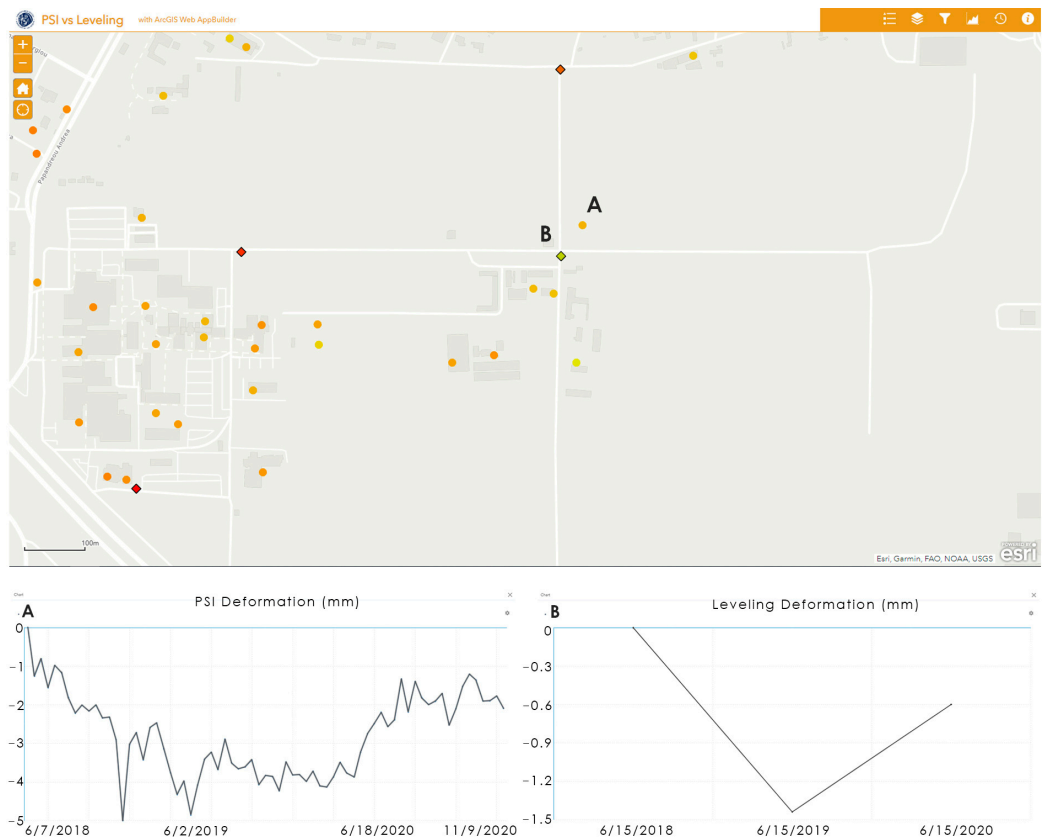


Figure 10. Example of displacement trends comparison via graphs, between PSI time series data (point A) and leveling data (point B), for the same time frame. Graph (A) shows subsidence trend from 17 June 2018 to 6 July 2019, relative stability trend from 6 July 2019 to 15 November 2019, and an uplift trend from 15 November 2019 to 27 December 2020. Graph (B) shows a subsidence trend from 15 June 2018 to 15 June 2019 and an uplift trend from 15 June 2019 to 15 June 2020.

4.5. 3D Visualization of Vertical Displacement Tool

By using the 3D visualization of the vertical displacement tool, users have the option to inspect PSI time series over an area and temporal subset through a 3D map. Every inter-

mediate displacement PSI time series value is presented in tiles, including all 138 different dates in layers expanding on the z-axis from old (lower layers) to recent dates (upper layers). An example of this 3D visualization tool of PSI time series data is applied and presented in a subarea of interest, for a predefined period, in Figure 11. Each layer represents one specific date, starting from 10 April 2015 on the lowest layer and ending on the higher layer and the last date of 27 December 2020. For the examined period, displacement values vary from -28 mm up to 2.5 mm. The lowest values are present mostly in the SW part of the study area, which is characterized by subsidence. The rest of the study area is characterized by many random value fluctuations (mostly stable, with some low-level motion detected occasionally). Displacement seems to increase in the SW part of the study area towards the more recent dates, with maximum displacement average values of approximately 28 mm in the last two years (2019–2020).



Figure 11. A presentation of 3D visualization of PSI time series displacement values in Sindos Region from 2015 to 2020. The value for each date is presented as a tile in space. The orientation of image (a) is SE to NW, while that of image (b) is SN.

Another capability of this 3D visualization tool is to filter data by predefined time frame and value of displacement range by using slide bars, as shown in the example of Figure 12.

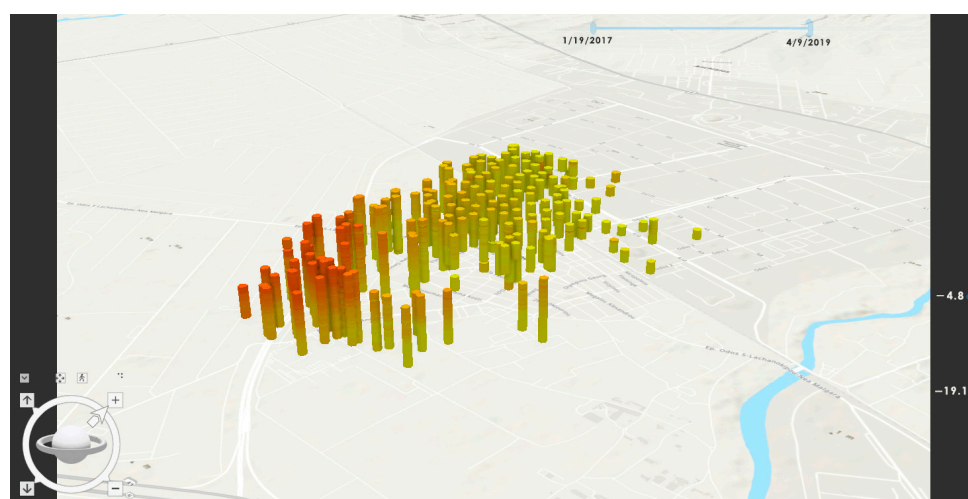


Figure 12. Tiles of displacement values after selection of time and value range. Values between 19 January 2017 and 9 April 2019, ranging from -19.1 mm to -4.8 mm, are presented in this example.

This 3D visualization tool also offers the capability to select one or more different points on multiple epochs and generate PSI time series graphs, which present the evolution of displacement, as shown in Figure 13.

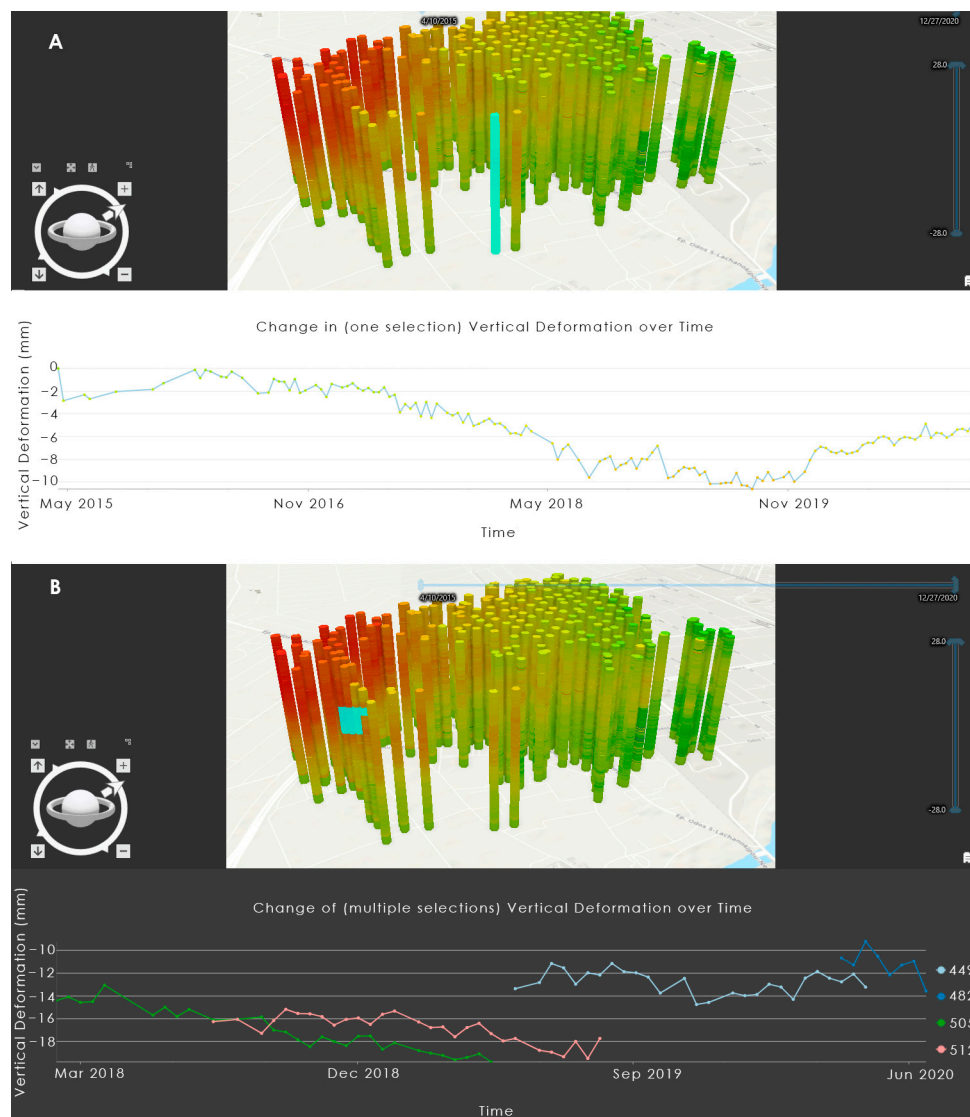


Figure 13. In image (A), a chart of the evolution of displacement values for one specific point is presented for the period between May 2015 and November 2020. All selected displacement values of the point are presented in blue color on the 3D map. In image (B), multiple selections of points (their displacement values) and dates are selected and presented on the chart, from March 2018 until June 2020. Displacement values of each selected record are depicted by different colored lines on the graph.

By using this cartographic tool, users not only have the option of visualizing and exploring PSI time series data in one 3D map but also generate graphs of the temporal evolution of each point of the dataset. With this capability, a comparison of deformation trends between various records of the dataset can be achieved. A limitation of this visualization 3D tool stems from the need to become an easily accessible web map application instead of being shared as a layer package.

4.6. Velocity Estimation Depending on Time Frame Tool

This visualization tool can be used for estimating mean velocity rates on smaller predefined areas and time frames. Moreover, by isolating and estimating mean velocity rates for a predefined subarea and a temporal frame, abrupt land displacement phenomena (e.g., landslides or earthquakes) can be studied and visualized. These phenomena would otherwise not have been properly presented through a large number of record time series

dataset visualization because of their smoother fluctuation through time. An example of the mean velocity estimation tool is presented in Figure 14.

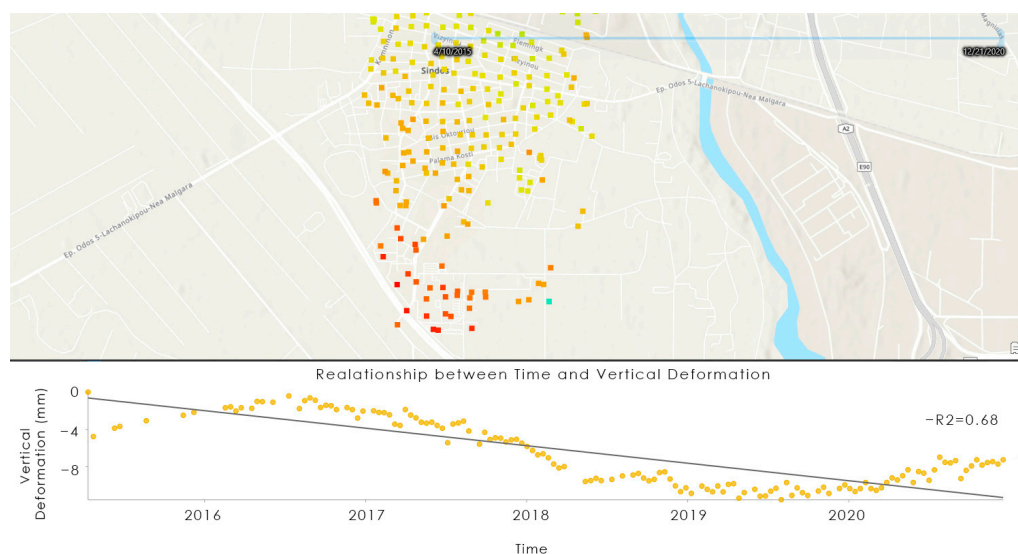


Figure 14. Mean velocity rates of Sindos region have been estimated and visualized for the period between 2015 and 2020. A graph of the PSI time series displacement values but also mean velocity is presented by the linear regression line for the selected record in the SE.

By estimating velocity rates of isolated temporal and spatial subareas, expert users have the option to visualize and compare them with the default dataset rates. A limitation arises from the need of downloading a supplementary file in order to use this cartographic tool. This file contains the script developed for estimating velocity rates for any temporal and spatial subset selected. This cartographic tool is also served as a layer package.

4.7. Geo-Visualization Toolset

This web application offers a cartographic toolbox for visualizing and exploring PSI vertical ground motions. Every cartographic element of this application has a different symbology, scale, time reference, and area of interest. Therefore, each element has, in general, a different purpose, contributing to an overall visualization and understanding of PSI displacement motions.

A preview of the toolset is presented in Figure 15. Users can access this web application through a desktop computer/laptop with internet access and a web browser. Every thumbnail of each cartographic element is selectable and linked with an application, tool, or video, respectively. Both laboratories that have been involved in this study are also presented and linked to this final application. The geo-visualization toolset is accessible by the link: <https://bit.ly/Geo-VisualizationPSIData> (accessed on 9 December 2022).

By studying PSI data, it is evident that the comparison between different pieces of research is rather challenging because of different cartographic representation approaches. A common cartographic approach to PSI measurements could lead to more efficient comparisons between different studies.

The PSI dataset referring to Northern Greece provided an excellent opportunity to utilize the geo-visualization toolset. We strongly believe that the whole study area should be continuously studied in order to have a full overview of the evolution of land displacement through the years and to be able to visualize and efficiently diffuse the results to the users and the general public. One way to achieve that is through the integration of specifically designed scientific tools, an example of which is proposed in this study. This temporal monitoring would have many environmental, educational, humanitarian, and economic implications. The quality of the results from Northern Greece suggests that a

similar approach can not only improve but also upscale the level of ground displacement phenomena research over large areas.

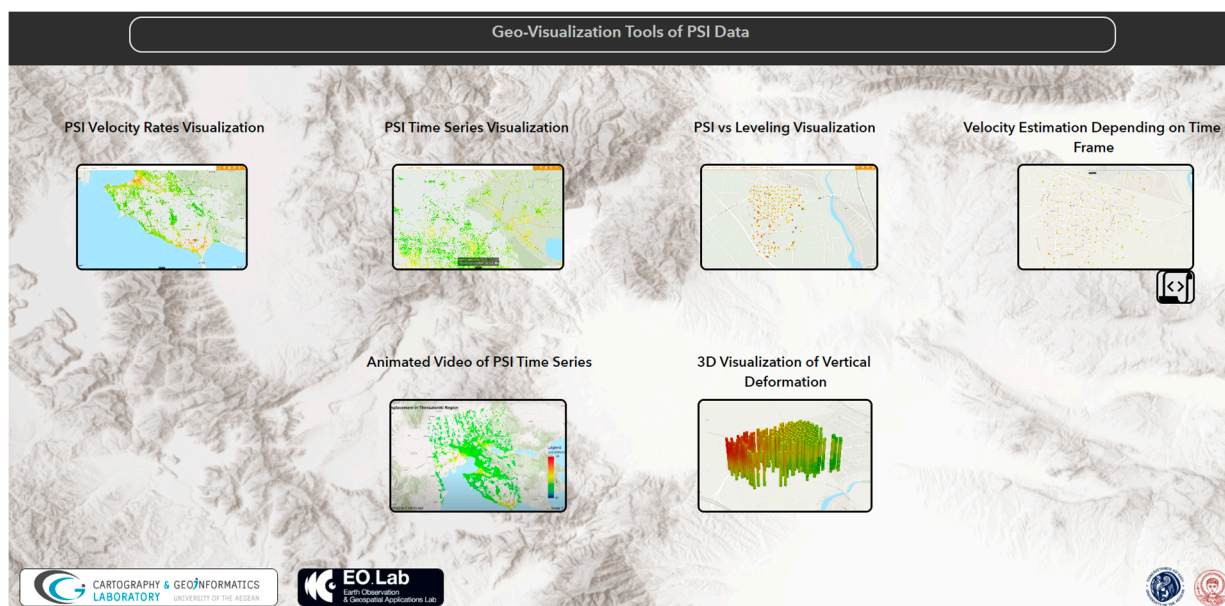


Figure 15. Geo-visualization toolset of all six cartographic elements created.

There is a large variety of different types of ground displacement [51,52]. Hence, it is suggested that the whole geo-visualization toolset should be further used on different study areas with different characteristics and types of displacement phenomena (e.g., landslides, earthquakes, volcanoes, etc.) or even in areas with the same mechanisms of displacement but with different rates and values so that tools are tested on a wide range of different conditions. All the geo-visualization toolset needs as input is a generic PSI export. Most PSI export data, such as EGMS's [26], etc., after some individual configurations for each application, could be used as inputs so that data could be explored and visualized through the visualization platform created (geo-visualization toolset).

In order to further expand the usage of the geo-visualization toolset, the idea of serving every individual cartographic tool under the terms of contextual cartography is being examined. By this approach, users do not need to have any knowledge about the cartographic theory, as everything is predefined within the applications and tools creation. All they have to do is describe their own context so they receive the corresponding cartographic results [53]. Data about ground displacement, such as urban land subsidence or the behavior of infrastructures, bridges, and dykes, has proven to be really helpful for city authorities, municipal departments, planners, infrastructure industries, mining industries, and non-governmental organizations (NGOs). However, it is usually difficult to provide that information to a “non-expert” user due to the intricacies of PS InSAR processing. Moreover, these parties are mostly interested in the final results rather than the complementary information [20]. In other words, users without cartographic experience can utilize a context-aware map application since the map is (or should be) accurately created by the application [53]. The main value of using contextual cartography in visualizing land displacement data is the fact that all data exported are fully used and served accordingly to each user's needs, saving time and pointless research through map layers and information.

5. Conclusions

To address the need for geo-visualization of PSI data, which are globally used for monitoring the dynamic phenomena of surface motion, a PSI geo-visualization toolset was developed. The combination of web map applications, interactive visualization tools, and animated maps shared on this geo-visualization toolset leads to the efficient exploration of

PSI data and provides useful information about the prevailing conditions in the study area in terms of ground motion.

More extensively:

- PSI velocity rates web map application contributes to efficient visualization of mean velocity rates of a study area. This web map application enables each user to interactively explore PSI velocity rates in detail, offering a variety of tools, including filtering, analyzing, and exporting subsets of the dataset.
- PSI time series web map application contributes to the visualization of the temporal evolution of deformation values. This web map application enables expert users to have a quick exploration of temporal PSI deformation values, as well as offering tools for filtering by date and exporting subsets of the dataset. For non-expert users, a temporal overview of PSI time series values is provided by the animated map.
- PSI versus leveling web map application contributes to the interactive comparison between PSI and leveling datasets. This web map application enables expert users to easily import leveling data (when available) in order to evaluate PSI measurements. Users also have the option of temporal exploration and comparison of both data sources by graph generation presenting trends of displacement.
- 3D visualization of the vertical displacement tool contributes to efficient visualization of the evolution of PSI time series values of displacements in one map. This visualization tool enables expert users to immediately explore PSI time series values by applying date and displacement value filters as well as to generate graphs of time series displacements. Utilizing the 3D visualization tool enables users to verify whether the evolution of PSI time series values is smooth and stable or even to detect and visualize any abrupt phenomena that occur.
- Velocity estimation of vertical displacement tool contributes to velocity estimation rate over different subareas and temporal subsets. By using this tool, expert users have the opportunity to isolate and explore abrupt phenomena by re-measuring velocity rates for those subareas as well as generating graphs of PSI time series evolution of data displacement.
- The combination of all those tools is about fulfilling each visualization need. Each of the cartographic applications, map tools, or animated map of the toolset could be tailored with mostly any generic PSI export data to provide a complete operational tool for interactive data visualization for each case study. Further research is mainly oriented on the investigation of scale issues (geographic, cartographic, spatial, and temporal) on efficient visualization of PSI fine resolution data, which will lead to the development of useful cartographic tools.

Author Contributions: Conceptualization, Panagiotis Kalaitzis, Christos Vasilakos, Antonios Mouratidis and Nikolaos Soulakellis; data curation, Michael Foumelis; investigation, Panagiotis Kalaitzis; methodology, Panagiotis Kalaitzis, Christos Vasilakos, Antonios Mouratidis and Nikolaos Soulakellis; supervision, Michael Foumelis, Christos Vasilakos and Nikolaos Soulakellis; visualization, Panagiotis Kalaitzis; writing—original draft, Panagiotis Kalaitzis and Antonios Mouratidis; writing—review and editing, Michael Foumelis, Christos Vasilakos and Nikolaos Soulakellis. All authors have read and agreed to the published version of the manuscript.

Funding: This research received no external funding.

Institutional Review Board Statement: Not applicable.

Informed Consent Statement: Not applicable.

Data Availability Statement: Not applicable.

Conflicts of Interest: The authors declare no conflict of interest.

References

- Konecny, M. Review: Cartography: Challenges and potential in the virtual geographic environments era. *Ann. GIS* **2011**, *17*, 135–146. [\[CrossRef\]](#)
- Taylor, D.R.F. Cartographic Visualization and Spatial Data Handling. In *Advances in GIS Research: Proceedings of the 6th International Symposium on Spatial Data Handling*; Waugh, T.C., Healey, R.G., Eds.; Taylor & Francis: London, UK, 1994; pp. 16–28.
- Cartwright, W.; Peterson, M.P. *Multimedia Cartography*; Springer: Berlin/Heidelberg, Germany, 1999; pp. 1–10.
- Neumann, A. Web mapping and web cartography. In *Springer Handbook of Geographic Information*; Springer: Berlin/Heidelberg, Germany, 2011; pp. 273–287.
- Zerdoumi, S.; Hashem, I.A.T.; Jhanjhi, N.Z. A New Spatial Spherical Pattern Model into Interactive Cartography Pattern: Multi-Dimensional Data via Geostrategic Cluster. *Multimed. Tools Appl.* **2022**, *81*, 22903–22952. [\[CrossRef\]](#) [\[PubMed\]](#)
- Norman, D. *Things That Make Us Smart: Defending Human Attributes in the Age of the Machine*; Diversion Books: New York, NY, USA, 2014.
- Buja, A.; Cook, D.; Swayne, D.F. Interactive High-Dimensional Data Visualization. *J. Comput. Graph. Stat.* **1996**, *5*, 78–99.
- Yi, J.S.; ah Kang, Y.; Stasko, J.; Jacko, J.A. Toward a Deeper Understanding of the Role of Interaction in Information Visualization. *IEEE Trans. Vis. Comput. Graph.* **2007**, *13*, 1224–1231. [\[CrossRef\]](#) [\[PubMed\]](#)
- Roth, R.E. Interacting with Maps: The Science and Practice of Cartographic Interaction. Ph.D. Thesis, University of Wisconsin–Madison, Madison, WI, USA, 2011; 215p.
- Roth, R.E. An Empirically-Derived Taxonomy of Interaction Primitives for Interactive Cartography and Geovisualization. *IEEE Trans. Vis. Comput. Graph.* **2013**, *19*, 2356–2365. [\[CrossRef\]](#)
- Bamler, R.; Hartl, P. Synthetic Aperture Radar Interferometry. *Inverse Probl.* **1998**, *14*, R1. [\[CrossRef\]](#)
- Li, F.; Liu, G.; Gong, H.; Chen, B.; Zhou, C. Assessing Land Subsidence-Inducing Factors in the Shandong Province, China, by Using PS-InSAR Measurements. *Remote Sens.* **2022**, *14*, 2875. [\[CrossRef\]](#)
- Crosetto, M.; Monserrat, O.; Cuevas-González, M.; Devanthéry, N.; Luzi, G.; Crippa, B. Measuring Thermal Expansion Using X-Band Persistent Scatterer Interferometry. *ISPRS J. Photogramm. Remote Sens.* **2015**, *100*, 84–91. [\[CrossRef\]](#)
- Osmanoğlu, B.; Dixon, T.H.; Wdowinski, S.; Cabral-Cano, E.; Jiang, Y. Mexico City Subsidence Observed with Persistent Scatterer InSAR. *Int. J. Appl. Earth Obs. Geoinf.* **2011**, *13*, 1–12. [\[CrossRef\]](#)
- Perissin, D.; Wang, T. Time-Series InSAR Applications Over Urban Areas in China. *IEEE J. Sel. Top. Appl. Earth Obs. Remote Sens.* **2011**, *4*, 92–100. [\[CrossRef\]](#)
- Sousa, J.J.; Hooper, A.J.; Hanssen, R.F.; Bastos, L.C.; Ruiz, A.M. Persistent Scatterer InSAR: A Comparison of Methodologies Based on a Model of Temporal Deformation vs. Spatial Correlation Selection Criteria. *Remote Sens. Environ.* **2011**, *115*, 2652–2663. [\[CrossRef\]](#)
- Sun, H.; Zhang, Q.; Zhao, C.; Yang, C.; Sun, Q.; Chen, W. Monitoring Land Subsidence in the Southern Part of the Lower Liaohe Plain, China with a Multi-Track PS-InSAR Technique. *Remote Sens. Environ.* **2017**, *188*, 73–84. [\[CrossRef\]](#)
- Blasco, J.M.D.; Fomelis, M.; Stewart, C.; Hooper, A. Measuring Urban Subsidence in the Rome Metropolitan Area (Italy) with Sentinel-1 SNAP-StaMPS Persistent Scatterer Interferometry. *Remote Sens.* **2019**, *11*, 129. [\[CrossRef\]](#)
- Fomelis, M.; Delgado Blasco, J.M.; Brito, F.; Pacini, F.; Pishchvar, P. Snapping for Sentinel-1 Mission on Geohazards Exploitation Platform: An Online Medium Resolution Surface Motion Mapping Service. In Proceedings of the International Geoscience and Remote Sensing Symposium (IGARSS), Brussels, Belgium, 11–16 July 2021.
- Gehlot, S.; Hanssen, R.F. Monitoring and interpretation of urban land subsidence using radar interferometric time Series and multi-source GIS database. In *Remote Sensing and GIS Technologies for Monitoring and Prediction of Disasters*; Springer: Berlin/Heidelberg, Germany, 2008; pp. 137–148.
- Van der Horst, T.; Rutten, M.M.; van de Giesen, N.C.; Hanssen, R.F. Monitoring Land Subsidence in Yangon, Myanmar Using Sentinel-1 Persistent Scatterer Interferometry and Assessment of Driving Mechanisms. *Remote Sens. Environ.* **2018**, *217*, 101–110. [\[CrossRef\]](#)
- Papoutsis, I.; Kontoes, C.; Alatza, S.; Apostolakis, A.; Loupasakis, C. InSAR Greece with Parallelized Persistent Scatterer Interferometry: A National Ground Motion Service for Big Copernicus Sentinel-1 Data. *Remote Sens.* **2020**, *12*, 3207. [\[CrossRef\]](#)
- Pumpuang, A.; Aobpaet, A. The Comparison of Land Subsidence between East and West Side of Bangkok, Thailand. *Built Environ. J.* **2020**, *17*, 1–9. [\[CrossRef\]](#)
- Abubakar, S.; Aravind, A.; Shanmugaveloo, L. Surface Deformation Studies in South of Johor Using the Integration of InSAR and Resistivity. *CaJoST* **2021**, *3121*, 167–172.
- Zhang, X.; Feng, M.; Zhang, H.; Wang, C.; Tang, Y.; Xu, J.; Yan, D.; Wang, C. Detecting Rock Glacier Displacement in the Central Himalayas Using Multi-Temporal Insar. *Remote Sens.* **2021**, *13*, 4738. [\[CrossRef\]](#)
- Kotzerke, P.; Siegmund, R.; Langenwalter, J. *End-To-End Implementation and Operation of the European Ground Motion Service (EGMS)*; Technical Report EGMS-D3-ALG-SC1-2.0-006; European Environment Agency: Copenhagen, Denmark, 2022.
- Bredal, M.; Dehls, J.; Larsen, Y.; Marinkovic, P.; Lauknes, T.R.; Stødle, D.; Moldestad, D.A. The Norwegian National Ground Motion Service (InSAR.No): Service Evolution. In Proceedings of the AGU Fall Meeting, San Francisco, CA, USA, 9–13 December 2019; p. G13C-0559.
- Mountrakis, D. *Geology and Geotectonic Evolution of Greece*; University Studio Press: Thessaloniki, Greece, 2010.

29. Tranos, M.D.; Papadimitriou, E.E.; Kiliyas, A.A. Thessaloniki—Gerakarou Fault Zone (TGFZ): The Western Extension of the 1978 Thessaloniki Earthquake Fault (Northern Greece) and Seismic Hazard Assessment. *J. Struct. Geol.* **2003**, *25*, 2109–2123. [[CrossRef](#)]
30. Meinhold, G.; Kostopoulos, D.K. The Circum-Rhodope Belt, Northern Greece: Age, Provenance, and Tectonic Setting. *Tectonophysics* **2013**, *595–596*, 55–68. [[CrossRef](#)]
31. Raspini, F.; Loupasakis, C.; Rozos, D.; Moretti, S. Advanced Interpretation of Land Subsidence by Validating Multi-Interferometric SAR Data: The Case Study of the Anthemountas Basin (Northern Greece). *Nat. Hazards Earth Syst. Sci.* **2013**, *13*, 2425–2440. [[CrossRef](#)]
32. Svirgkas, N.; Papoutsis, I.; Loupasakis, C.; Kontoes, C.; Kiratzi, A. Geo-Hazard Monitoring in Northern Greece Using InSAR Techniques: The Case Study of Thessaloniki. In Proceedings of the 9th International Workshop Fringe, Frascati, Italy, 23–27 March 2015; Volume 731. [[CrossRef](#)]
33. Costantini, F.; Mouratidis, A.; Schiavon, G.; Sarti, F. Advanced InSAR Techniques for Deformation Studies and for Simulating the PS-Assisted Calibration Procedure of Sentinel-1 Data: Case Study from Thessaloniki (Greece), Based on the Envisat/ASAR Archive. *Int. J. Remote Sens.* **2016**, *37*, 729–744. [[CrossRef](#)]
34. Elias, P.; Benekos, G.; Perrou, T.; Parcharidis, I. Spatio-Temporal Assessment of Land Deformation as a Factor Contributing to Relative Sea Level Rise in Coastal Urban and Natural Protected Areas Using Multi-Source Earth Observation Data. *Remote Sens.* **2020**, *12*, 2296. [[CrossRef](#)]
35. Holdahl, S.R.; Morrison, N.L. Regional Investigations of Vertical Crustal Movements in the US, Using Precise Relevelings and Mareograph Data. *Tectonophysics* **1974**, *23*, 373–390. [[CrossRef](#)]
36. Nakano, T.; Matsuda, I. A Note on Land Subsidence in Japan. *Geogr. Rep. Tokyo Metropol. Univ.* **1976**, *11*, 147–162.
37. Dong, H.; Gu, D.; Li, G.; Zhang, L.; Chen, S.Y.; Wang, W.L. *Research on Vertical Recent Crustal Movement of the Mainland of China*; Xi'an Carto2 Graphic Publishing House: Xi'an, China, 2002.
38. Cigna, F.; Esquivel Ramírez, R.; Tapete, D. Accuracy of Sentinel-1 PSI and SBAS InSAR Displacement Velocities against GNSS and Geodetic Leveling Monitoring Data. *Remote Sens.* **2021**, *13*, 4800. [[CrossRef](#)]
39. Morgan, J.D.; Eddy, B.; Coffey, J.W. Activating Student Engagement with Concept Mapping: A Web GIS Case Study. *J. Geogr. High. Educ.* **2022**, *46*, 128–144. [[CrossRef](#)]
40. Degbelo, A. FAIR Geovisualizations: Definitions, Challenges, and the Road Ahead. *Int. J. Geogr. Inf. Sci.* **2022**, *36*, 1059–1099. [[CrossRef](#)]
41. Gardner Oldemeyer, T.A.; Russell, G.P. Interactive Web Mapping Tools and Custom Subsurface Cross-Sections for Interdisciplinary Geologic Investigation. *Appl. Comput. Geosci.* **2022**, *13*, 100077. [[CrossRef](#)]
42. Gehlot, S.; Perski, Z.A.; Hanssen, R. Web-Based Framework for Ps-InSAR Data Interpretation Assisted By Geo-Spatial Information Fusion. In Proceedings of the ISPRS Mid-term Symposium, 'Remote Sensing: From Pixels to Processes', Enschede, The Netherlands, 8–11 May 2006; pp. 2–5.
43. Kraak, M.; Edsall, R.; MacEachren, A.M. Cartographic Animation and Legends for Temporal Maps: Exploration and or Interaction. In Proceedings of the 18th International Cartographic Conference, Stockholm, Sweden, 23–27 June 1997; pp. 1–8.
44. Aobpaet, A.; Cuenca, M.C.; Hooper, A.; Trisiriatayawong, I. InSAR Time-Series Analysis of Land Subsidence in Bangkok, Thailand. *Int. J. Remote Sens.* **2013**, *34*, 2969–2982. [[CrossRef](#)]
45. Karimzadeh, S.; Cakir, Z.; Osmanoğlu, B.; Schmalzle, G.; Miyajima, M.; Amiraslazadeh, R.; Djamour, Y. Interseismic Strain Accumulation across the North Tabriz Fault (NW Iran) Deduced from InSAR Time Series. *J. Geodyn.* **2013**, *66*, 53–58. [[CrossRef](#)]
46. ESA WorldCover. Available online: <https://esa-worldcover.org/en> (accessed on 22 February 2022).
47. Doukas, I.; Ifadis, I.; Savvaidis, P. *Monitoring and Analysis of Ground Subsidence Due to Water Pumping in the Area of Thessaloniki, Hellas*; Aristotle University of Thessaloniki: Thessaloniki, Greece, 2004; pp. 1–14.
48. Psimoulis, P.; Ghilardi, M.; Fouache, E.; Stiros, S. Subsidence and Evolution of the Thessaloniki Plain, Greece, Based on Historical Leveling and GPS Data. *Eng. Geol.* **2007**, *90*, 55–70. [[CrossRef](#)]
49. Raucoules, D.; Parcharidis, I.; Feurer, D.; Novalli, F.; Ferretti, A.; Carnec, C.; Lagios, E.; Sakkas, V.; Le Mouelic, S.; Cooksley, G.; et al. Ground Deformation Detection of the Greater Area of Thessaloniki (Northern Greece) Using Radar Interferometry Techniques. *Nat. Hazards Earth Syst. Sci.* **2008**, *8*, 779–788. [[CrossRef](#)]
50. Mouratidis, A.; Albanakis, K. Hypsometric Changes Near Kavallari Based on Multi-Temporal Dems and Extensive Gns Measurements. In Proceedings of the 9th Geographical Conference of Greece, Athens, Greece, 5–7 November 2010; pp. 116–123.
51. Berti, M.; Corsini, A.; Franceschini, S.; Iannacone, J.P. Automated Classification of Persistent Scatterers Interferometry Time Series. *Nat. Hazards Earth Syst. Sci.* **2013**, *13*, 1945–1958. [[CrossRef](#)]
52. Mirmazloumi, S.M.; Wassie, Y.; Navarro, J.A.; Palamà, R.; Krishnakumar, V.; Barra, A.; Cuevas-González, M.; Crosetto, M.; Monserrat, O. Classification of Ground Deformation Using Sentinel-1 Persistent Scatterer Interferometry Time Series. *GISci. Remote Sens.* **2022**, *59*, 374–392. [[CrossRef](#)]
53. Kozel, J.; Štampach, R. Practical Experience with a Contextual Map Service. In *Geographic Information and Cartography for Risk and Crisis Management. Lecture Notes in Geoinformation and Cartography*; Konecny, M., Zlatanova, S., Bandrova, T., Eds.; Springer: Berlin/Heidelberg, Germany, 2010; pp. 305–316. [[CrossRef](#)]

Disclaimer/Publisher's Note: The statements, opinions and data contained in all publications are solely those of the individual author(s) and contributor(s) and not of MDPI and/or the editor(s). MDPI and/or the editor(s) disclaim responsibility for any injury to people or property resulting from any ideas, methods, instructions or products referred to in the content.